A biphasic metabolism-β-lactamase production landscape governs the inoculum effect in β-lactamase-expressing *Escherichia coli.*

Ariane R. Kalifa Torjeman[1,2], Kielan Singh[2], Philopatier Ibrahim[2], Trent Moulder[2], Naziba Nuha[2], Julia Gumirov[2], Tiffany Rakela[1,2,3], Debora Pereira Mcmenamin[1,3], Daniel Winget[3], Taija White[3], Archit Pipalva[3], Allison. J. Lopatkin[4,5,6], and Robert P. Smith[1,3]

1. Cell Therapy Institute, Kiran Patel College of Allopathic Medicine, Nova Southeastern University, Fort Lauderdale, FL, 33314
2. Department of Biological Sciences, Halmos College of Arts and Sciences, Nova Southeastern University, Fort Lauderdale, FL, 33314
3. Department of Medical Education, Kiran Patel College of Allopathic Medicine, Nova Southeastern University, Fort Lauderdale, FL, 33314
4. Department of Chemical Engineering, University of Rochester; Rochester, NY 14627; USA
5. Department of Microbiology and Immunology, University of Rochester Medical Center; Rochester, NY 14627; USA
6. Department of Biomedical Engineering, University of Rochester Medical Center; Rochester, NY 14627; USA

Correspondence should be addressed to Robert P. Smith. E-mail: rsmith@nova.edu

Keywords: inoculum effect, β-lactamase, growth rate, metabolism, density-dependent, β-lactam

Abstract

The inoculum effect (IE) reduces the efficacy of antibiotics both *in vitro* and in clinical settings. However, we do not understand, nor can we predict, when IE will occur. Recent work has shown that interactions between bacterial metabolism and growth explain IE in bacteria that lack acquired resistance, such as β-lactamases. Owing to the energetic costs associated with production, the expression of β-lactamases can perturb metabolism and growth rate, which may impact their relationship with IE. Indeed, the presence of a β-lactamase does not guarantee IE, suggesting additional aspects of bacterial physiology are at play. Using *Escherichia coli* expressing the NDM-1 β-lactamase, we quantified [ATP], growth rate, β-lactamase expression, and IE across multiple environments defined by the chemical composition of the growth medium. We found that expression of β-lactamases nonlinearly impacted both [ATP] and growth rate, but neither alone could predict IE. Instead, we found that the ratio of [ATP] to growth rate formed a biphasic relationship with the strength of IE. Mathematical modeling suggests that IE initially increases with the ratio of [ATP] to growth rate due to increased β-lactamase expression, which increasingly protects the population from antibiotics. However, once metabolism becomes sufficiently high, the ability of β-lactamases to protect the population is reduced, which decreases IE. Our results suggest that the chemical composition of the environment influences IE in β-lactamase-expressing bacteria, potentially resolving conflicting reports on the clinical relevance of IE. They may also aid in developing strategies to predict, prevent, and minimize IE.

Introduction

It has long been observed that the density of a bacterial population can lead to antibiotic tolerance or resistance. This phenomenon, called the inoculum effect (IE), has been observed for nearly all bacteria and antibiotics [1-4]. For a given concentration of antibiotics, a population with a high density will survive antibiotic treatment and grow. However, if the population density is sufficiently low, the population is susceptible to the antibiotic and dies. Reports from the clinic have demonstrated that IE can increase the morbidity and mortality rates of patients by reducing antibiotic efficacy [5-7] and can drive the evolution of additional resistance mechanisms [8,9]. Despite being first reported in 1949[10], we currently lack approaches to identify and mitigate IE in the clinic.

While direct antibiotic-antibiotic target effects were thought to be the predominant mechanism governing antibiotic lethality, bacterial metabolism and growth rate are increasingly recognized as having a fundamental impact on determining antibiotic efficacy. Multiple studies have shown that increasing bacterial metabolism increases the lethality of antibiotics [11]. Bacterial growth has been shown to increase [12] and decrease [13] antibiotic lethality. Recent evidence has demonstrated that, for multiple Gram-negative bacteria and antibiotics, IE is dependent on both metabolism and growth rate [14,15]. In the absence of an acquired form of antibiotic resistance, increasing bacterial metabolism relative to growth rate decreases IE [16]. Here, high-density populations experience only a brief log phase, during which metabolism and thus antibiotic lethality are greatest, before entering the stationary phase, where both are reduced. Owing to only a brief log phase, this enables the high-density population to tolerate higher concentrations of antibiotics. In contrast, low-density populations remain in the log phase for a longer period before entering the stationary phase, making them more susceptible to antibiotics. The growth rate dictates how fast each population reaches a stationary state, with a faster growth rate providing more protection due to its ability to reduce the

time spent during the log phase. Together, differences in antibiotic tolerance between the high- and low-density populations, owing to these dynamics, determine IE.

The notion that both metabolism and growth rate determine IE is interesting in light of multiple studies that have identified the presence of a β-lactamase as a key determinant of IE [3,5]. β-lactamases are enzymes that render β-lactam antibiotics inactive, thus conferring resistance [17]. IE in β-lactamase-expressing bacteria has been associated with antibiotic failure in the clinic and has been reported as a risk factor in determining 30-day mortality [18-20]. Expression of heterologous proteins, including β-lactamases, has well-documented effects on both metabolism and growth rate [21]. Transcription, translation, and enzymatic activity of upregulated and overexpressed proteins can cause bacteria to alter ATP production [22] and can reduce [ATP] available for other cellular processes [21]. This often manifests as a reduction in growth rate [23,24]. As β-lactamases have the potential to alter metabolism and growth rate, the ability of these two facets of cell physiology to determine IE may be changed.

One hypothesis to explain IE in β-lactamase-expressing bacteria is the collective inactivation of β-lactams. Here, the higher the density of bacteria, the more β-lactam can be inactivated by the collective β-lactamase activity of all members of the population (Fig. 1A)[25]. As populations with higher density will inactivate more antibiotic than their lower density counterparts[25-29], the higher density population will only succumb to the antibiotic at a greater concentration, giving rise to IE. This collective inactivation not only reduces antibiotic efficacy but also facilitates the growth of non-resistant bacteria[25], alters selection dynamics[29], and can maintain polymicrobial infection resiliency during antibiotic treatment[30]. However, the presence of a β-lactamase does not necessarily guarantee IE, as many strains containing a β-lactamase do not show IE[31,32]. Even in the presence of β-lactamases, the strength of IE can vary depending on the type of β-lactam antibiotic, ranging from severe to none

at all [33]. Evidence from the clinic has shown that not all β-lactamase-positive isolates have IE against the same antibiotic, even when controlling for β-lactamase type and bacterial species [5]. Together, this suggests that additional aspects of cellular physiology, such as metabolism and growth, may determine IE in β-lactamase-expressing bacteria. While this is plausible, it has yet to be tested. Accordingly, it remains unclear how the expression of a β-lactamase alters the relationship between metabolism, growth, and IE. Addressing this open question may help define growth environments where IE is amplified, reduced, or eliminated, which in turn may help address conflicting data surrounding the perceived clinical importance of IE [34] and drive the development of interventions that reduce the severity and occurrence of IE in the clinic.

Results

An experimental approach to quantifying the effect of metabolism and growth rate on IE in β-lactamase-expressing bacteria.

To understand how bacterial metabolism, growth rate, and β-lactamase expression would determine IE, we used a strain of *Escherichia coli* that produces the NDM-1 β-lactamase[35] from a medium copy number plasmid and under the regulation of an isopropyl-β-D-thiogalactopyranoside (IPTG) inducible promoter, $P_{lac/ara-1}$[36] (Fig. 1B). We chose to use the NDM-1 β-lactamase given its clinical relevance, global distribution, and ability to inactivate a wide range of β-lactams, including carbapenems[37]. Previous work has shown that the type of carbon source can influence both metabolism[38] and growth rate[39]. Accordingly, to manipulate both metabolism and growth rate, we grew bacteria in minimal medium containing a carbon source, which defined the growth environment. We also provided casamino acids, which served as a nitrogen source (Fig. 1C). For a given carbon source, we supplied three different percentages of casamino acids (0.1, 0.5, and 1%). Averaging across all three percentages thus allows us to identify a generalizable carbon source-dependent effect on

bacterial metabolism and growth rate, yielding a single value for a given growth environment. To vary the expression of NDM-1, we provided different [IPTG] in the growth medium, an approach that has been previously observed to change the expression of elements downstream of the $P_{lac\text{-}ara\text{-}1}$ promoter [36].

While multiple facets of bacterial metabolism can be measured, we focused on [ATP] due to its well-defined relationship with antibiotic lethality and its significant correlation with other measures of metabolism in bacteria, including NAD^+/NADH and oxygen consumption rate[14], including in IE [16]. To measure [ATP], we used a previously published method that measures bacterial metabolism separate from any changes in growth rate[14]. To measure growth rate, we made high-resolution measurements of cell density (OD_{600}) in a microplate reader without antibiotics. We then used a custom-built model to estimate the maximum growth rate by fitting a logistic growth curve through the resulting experimental growth curve[16]. Finally, to measure the expression of β-lactamase, we replaced NDM-1 with a green fluorescent protein (GFP); thus, GFP was driven by the same promoter using the same plasmid backbone, serving as a reliable surrogate of NDM-1 expression. Together, this approach allowed us to measure bacterial metabolism (ATP), growth rate, and β-lactamase expression for a given growth environment.

Increasing the expression of the NDM-1 β-lactamase alters [ATP] and growth rate.

To start, we measured the effect of increasing [IPTG] on GFP-expression. When grown in M9 medium with glucose as a carbon source, we found that as [IPTG] increased, the amount of GFP per cell significantly increased, confirming the inducible and dose-dependent nature of our expression system (Fig. 1D). We did not find a significant difference in GFP signal normalized by initial cell density (Supplementary Fig. 2), suggesting that initial density does not impact the *per-cell* expression of NDM-1. Next, we measured [ATP] normalized by cell density in medium with increasing [IPTG]

in our NDM-1 expressing strain. We found that with 1 mM IPTG, [ATP] per cell was significantly greater compared to the 0 mM IPTG control (Fig. 1E). We also found that expression of NDM-1 with 0.1 mM IPTG reduced [ATP] per cell relative to both 0.3 mM and 1 mM IPTG, indicative of a non-linear relationship between [ATP] and NDM-1 induction. Consistent with literature showing that expression from low-copy-number plasmids may not result in changes to growth [40], we found no significant differences in growth rate with increasing [IPTG] (Fig. 1F). Finally, we measured log[ATP]/growth rate for each [IPTG], a metric that we previously observed correlated with IE[16], and found that as [IPTG] increased, so did log[ATP]/growth rate (Fig. 1G). Taken together, we found that increasing [IPTG] in M9 medium with glucose increased expression of GFP, but had non-linear effects on bacterial metabolism and growth rate.

A simple mathematical model predicts the effects of β-lactamase, metabolism, and growth on IE.

To guide our experiments and provide insight into how growth and metabolism might impact IE, we created a simple mathematical model (see *Methods*, Eq. 1). Our model comprises two terms that govern bacterial growth and death. The density of the bacteria population (N) follows logistic growth, scaled by growth rate (μ) and metabolism (ε), where ε approximates a maintenance coefficient representing energy that is not used for biomass. A modified Michaelis-Menton equation captures antibiotic-driven *per capita* death; death depends on the population density (N), the antibiotic concentration (A), bacterial metabolism (ε), and the antibiotic killing rate (b). However, *per capita* death rate can be reduced by the production of β-lactamases (β), which is scaled by population density (N). This scaling captures a previous hypothesis that suggests the more bacteria in the population, the more β-lactamases are produced, and the more antibiotics can be inactivated[25]. Whether the population survives or collapses for a given concentration of antibiotic (A) depends on the balance between

logistic growth (driven by growth (μ) and metabolism (ε)) and *per capita* antibiotic death, which is reduced as both β-lactamase expression (β) and population density (N) increase.

To test the predictive ability of our model, we initiated simulations using two initial densities of bacteria with increasing β-lactamase expression, but with fixed values of metabolism and growth rate. Our simulations predict that increasing β-lactamase expression increases IE (Fig. 2A), which we measured as the difference in the minimum inhibitory concentration (MIC) between bacterial populations initiated from high and low densities (henceforth referred to as ΔMIC). When $\beta = 1$, the high-density population grows at greater values of antibiotic as compared to the low-density population, predicting the defining feature of IE (Fig. 2B). Increasing β-lactamase expression ($\beta = 3$) increases the difference in the range of antibiotics over which the high-density population survives, which increases ΔMIC.

To test these predictions, we first measured ΔMIC for NDM-1 expressing bacteria in medium with glucose and either 0 mM or 0.1 mM [IPTG]. We chose these conditions as experiments show that significant differences in [ATP] and growth rate are not observed (Fig. 2C), but that 0.1 mM IPTG increases expression of NDM-1 (Fig. 2D). To determine ΔMIC, we challenged NDM-1 expressing bacteria with the β-lactam antibiotic ampicillin, as it is often used to develop mechanisms of antibiotic resistance[41]. We used two initial densities of bacteria: a high-density population ($5.3 \times 10^5 \pm 1.14 \times 10^5$ CFU/mL) and a low-density population ($2.34 \times 10^4 \pm 2.88 \times 10^3$ CFU/mL). We calculated ΔMIC by determining the difference between the MICs of the high- and low-initial-density populations. ΔMIC was significantly greater when bacteria were provided with 0.1 mM IPTG (Fig. 2D), confirming our modeling predictions that increased NDM-1 expression leads to increased ΔMIC.

Next, we performed simulations holding β-lactamase expression constant, but increasing the ratio of metabolism to growth rate. Consistent with previous work[16], increasing metabolism/growth

rate (e.g., ε/μ) decreases ΔMIC (Fig. 2E). For example, increasing metabolism/growth rate from 0.03 to 0.05 shrinks the range of antibiotic over which the high density, but not the low density, population grows. This reduces ΔMIC (Fig. 2F). To verify these predictions, we quantified [ATP] and growth rate in NDM-1 expressing bacteria grown in medium with adenine and without [IPTG]. As compared to bacteria grown in glucose, providing adenine increased both [ATP] and growth rate, which increased [ATP]/growth rate (Fig. 2G). While we did not find any differences in GFP expression between these two conditions, ΔMIC was significantly smaller when adenine was the carbon source (Fig. 2H). Consistent with our model predictions, this demonstrated that increasing log[ATP]/growth rate reduced ΔMIC. Taken together, our simple mathematical model could capture the behaviors of our experimental system.

Our model predicts biphasic dependence of ΔMIC on metabolism and growth.

Using our model, we determined ΔMIC for a range of metabolism and β-lactamase expression values, while keeping growth rate constant (Fig. 3A). We found that combinations of β-lactamase expression and metabolism led to a range of ΔMIC. Slices through the simulated landscape provided insight into the relationship between metabolism and β-lactamase expression on ΔMIC (Fig. 3B). Our model predicts that if β-lactamase expression increases relatively faster than metabolism (ε), ΔMIC forms a biphasic relationship with metabolism /growth rate. Here, ΔMIC first increases with increasing metabolism/growth rate, whereupon further increases in metabolism/growth rate reduce ΔMIC. The relative increase in β-lactamase expression governs the prominence of the peak of this relationship; larger increases in β-lactamase expression relative to metabolism lead to a greater prominence. However, if metabolism increases relatively faster than β-lactamase expression, ΔMIC decreases with increasing metabolism/growth rate. These general trends in the simulated landscape

were consistent across a range of model parameters (Supplementary Fig. 4), demonstrating the robustness of these predictions. This biphasic relationship is also dependent on changes in both β-lactamase and metabolism, as increasing one, but not the other, leads to an increase or decrease in ΔMIC, respectively (Supplementary Fig. 4).

Our quantification of NDM-1 expression, [ATP], and growth rate in medium with glucose provided only a limited parameter space in the large simulated landscape predicted by our model. To expand the combination of NDM-1 expression, [ATP], and growth rate, we grew bacteria in minimal medium with three additional carbon sources: ribose, adenine, and acetate, which have been shown to alter [ATP] and growth rate[16]. Using the GFP-expressing strain of *E. coli*, we found that increasing [IPTG] consistently increased GFP in ribose (Fig. 3C). However, for adenine and acetate, while [IPTG] increased GFP relative to the no IPTG control, the amount of GFP produced did not necessarily increase with increasing [IPTG]. Similar to our findings with glucose (Fig. 1E), quantification of [ATP] using these carbon sources revealed a wide range of significant differences within each carbon source (Fig. 3D); in nearly all cases, including [IPTG] in the medium significantly increased [ATP], suggesting that NDM-1 expression impacts bacterial metabolism. In contrast, relatively few significant differences in growth rate were observed (Fig. 3E). While increasing [IPTG] altered the growth rate for both adenine and ribose, no significant differences were observed for acetate. These carbon source-specific trends in [ATP] and growth rate provided a wide range of log[ATP]/growth rate values (Fig. 3F). Coupled with carbon source-dependent effects on β-lactamase expression, the use of different carbon sources provided a large parameter space over which we could understand the interdependence of β-lactamase expression, [ATP], and growth rate.

ΔMIC forms a biphasic relationship with log[ATP]/growth rate.

Using glucose, adenine, ribose, and acetate as carbon sources, we quantified ΔMIC using populations initiated from high and low densities (Fig. 4A). Uninduced cultures had a relatively small ΔMIC, which can be attributed to the endogenous *ampC* β-lactamase and/or IE resulting from metabolic and growth dynamics alone[16]. We found that increasing [IPTG] in the growth medium consistently and significantly increased ΔMIC relative to the uninduced control, suggesting that IE in our bacteria is mainly due to NDM-1, with *ampC* having a negligible impact. With glucose, ribose, or acetate, increasing [IPTG] significantly increased ΔMIC. However, with adenine, there were no significant differences in ΔMIC amongst all [IPTG] used.

We then plotted ΔMIC for all carbon sources and [IPTG] as a function of log[ATP]/growth rate. Consistent with our modeling predictions, we found a biphasic dependence of ΔMIC on log[ATP]/growth rate; increasing ΔMIC first increased with log[ATP]/growth rate and peaked at an intermediate range of log[ATP]/growth rate. Further increases in log[ATP]/growth rate resulted in reductions in ΔMIC. Fitting the data with a Gaussian curve yielded a relatively high R^2 value (0.86) and significance across all three measures of fit (peak value, critical point, and growth rate). While both plots of log[ATP] and growth rate as a function of ΔMIC also fit a Gaussian curve, their R^2 values were markedly less (R^2 = 0.48 and 0.11, respectively, Supplementary Fig. 8). Linear regression analysis showed that neither [ATP] nor growth rate alone could predict ΔMIC (Supplementary Fig. 8).

Importantly, the biphasic relationship between ΔMIC and log[ATP]/growth rate was only observed when NDM-1 was expressed. Expression of GFP in place of NDM-1 resulted in a linear decreasing relationship between ΔMIC and log[ATP]/growth rate; as log[ATP]/growth rate increased, ΔMIC decreased. This finding was consistent with previous work, which showed that in the absence of an acquired form of resistance, ΔMIC decreases as a function of log[ATP]/growth rate[16].

Furthermore, while we found that GFP expression was weakly correlated with ΔMIC, the R^2 value was less than that of our Gaussian fit, suggesting that β-lactamase expression alone cannot fully account for the variance in ΔMIC ($R^2 = 0.36$, Fig. 4D). Taken together, our experiments coupled with modeling provide evidence that interactions between metabolism, growth, and β-lactamase expression determine IE in β-lactamase-expressing bacteria.

Discussion

We have shown that expressing a plasmid-borne β-lactamase can non-intuitively alter [ATP] while often leaving growth rate unchanged; together, altering log[ATP]/growth rate. Using diverse carbon sources, we found that ΔMIC exhibits biphasic dependence on log[ATP]/growth rate, where intermediate values of log[ATP]/growth rate led to the greatest strength of IE. Simulations suggest that this is due to interactions between metabolism, growth rate, and β-lactamase expression. This trend is β-lactamase-specific, as the expression of GFP abolished the biphasic relationship between log([ATP])/growth rate and ΔMIC.

We found that the expression of NDM-1 using IPTG generally served to increase [ATP], but otherwise reduced or had no impact on the growth rate (Fig. 3D and E). This suggests that the energetic costs of expressing NDM-1 can be decoupled from changes in growth rate depending upon the growth environment and expression rate. While it has been generally assumed that expression of heterologous proteins imposes a metabolic burden on the cell, including β-lactamases [23,24], manifesting as a reduction in growth rate [42], this may not always be the case, as presented here. Indeed, acquisition of some, but not all β-lactamases, can lead to an increase in growth rate, even in the absence of antibiotics[23]. To our knowledge, we are the first to demonstrate an increase in [ATP] resulting from β-lactamase expression. Increases in [ATP] due to heterologous protein expression have been reported elsewhere[43], and this may be attributed to a compensatory change in cellular respiration.

The observed biphasic relationship between ΔMIC and log[ATP]/growth demonstrates that IE is maximized at intermediate values of log[ATP]/growth. This observation can be explained by considering how log[ATP]/growth determines ΔMIC in the absence of a β-lactamase, and the influence of β-lactamase expression on ΔMIC. We previously demonstrated how the relationship between [ATP] and growth rate, which we called growth productivity, impacts IE [16]. Consider two populations of bacteria initiated from high and low densities growing in a closed system (Fig. 5A). The population initiated at high density spends a relatively short time in log phase growth, where metabolism is highest, before entering the stationary phase, where metabolism is reduced. The population from low initial density spends considerably more time in the log phase before entering the stationary phase. As the time during which metabolism is highest is longer in the low-density population, it is more susceptible to metabolism-potentiated antibiotic lethality [14], leading to a lower MIC. In contrast, the MIC of the high-density population is higher, having spent only a minimal time in log phase, largely shielding it from metabolism-potentiated antibiotic lethality. The growth rate determines how fast each population reaches the stationary phase; slower growth rates allow more time for both populations to remain in the log phase. Accordingly, environments that lead to fast growth relative to low ATP (i.e., low log[ATP]/growth) exacerbate IE, whereas those with slow growth relative to high ATP (i.e., high log[ATP]/growth rate) minimize IE (Fig. 5B). Indeed, in the absence of a β-lactamase, our data and simulations demonstrate this trend (Fig. 2E-H, Fig. 4C).

Expressing a β-lactamase partially alters this relationship. Increasing β-lactamase expression increases ΔMIC (Fig. 5C), which is supported by our data and simulations (Fig. 2A-D); the more β-lactamases produced, the more β-lactam antibiotics can be degraded, resulting in a greater ΔMIC for the population. We hypothesize that this can explain the left side of the biphasic trend; as expression of β-lactamases increases, it increases ΔMIC (Fig. 5D). As log[ATP]/growth rate is relatively low, the

difference in MIC between the high and low density populations is accentuated, increasing ΔMIC until it reaches a peak. However, further increases in log[ATP]/growth rate begin to reduce the difference in MIC between the high and low density populations. Here, increasing metabolism (ATP) relative to growth potentiates antibiotic lethality; both high- and low-density populations inactivate similar amounts of β-lactam antibiotics, reducing the difference in MIC and leading to a lower ΔMIC (Fig. 5D). We hypothesize that this explains the right side of the biphasic trend. Indeed, our simulations support this idea; without changes to both β-lactamase expression (β) and metabolism (ε)/growth rate (μ), a biphasic relationship is not observed (Supplementary Fig. 4). We cannot rule out reduced expression or dysfunctional β-lactamase functionality at high log[ATP]/growth rate, which may also explain the right side of this trend. However, we did not find a clear biphasic trend that correlated with the data points our plot of ΔMIC versus log[ATP]/growth rate when GFP was plotted as a function of log[ATP]/growth rate or log[ATP] (Supplementary Fig. 8). Differences in carbon source alone cannot explain the biphasic trend, as multiple carbon sources are represented on the left and right of the curve (Fig. 4B).

Our results show that the carbon source in the growth medium shapes β-lactamase-mediated IE. This highlights that nutrients in the growth environment, and not just the expression of β-lactamases, influence the strength of IE. This finding is consistent with previous work showing that the chemical composition of the growth environment can strongly influence antibiotic efficacy [44,45], often by manipulating bacterial metabolism to potentiate or reduce antibiotic lethality. Similarly, we found that changes in carbon source, along with NDM-1 expression, could alter bacterial metabolism (ATP, Fig. 3D). The discovery that the chemical composition of the growth environment influences ΔMIC may help explain why some clinical studies have failed to find IE [7,46]. In contrast, others have found a pronounced effect on patient outcomes, including mortality [47,48]. It also suggests that different

infection sites may be more prone to IE than others, as the chemical composition of each site can vary in nutrients available to fuel bacteria [49,50]. Finally, it may explain why the presence of a β-lactamase alone cannot predict the occurrence of IE[31,32], as IE may only be present in specific growth environments. Defining growth environments where IE is amplified or diminished may improve predictions of antibiotic efficacy *in vivo*.

In conclusion, our study demonstrates that in β–lactamase–expressing *E. coli*, the strength of IE exhibits a biphasic dependence on log([ATP])/growth rate. These findings suggest that shifting the infection environment away from the intermediate "sweet spot" where IE is maximized using metabolic adjuvants or nutrient manipulations that affect bacterial metabolism and growth rate, may reduce IE, improving antibiotic efficacy and patient outcomes. Moreover, the development and subsequent monitoring of proxies of bacterial ATP, growth rate, and β-lactamase expression could help identify infection sites or patients that are more likely to have IE.

Methods

Bacterial strains, growth conditions, and antibiotics

E. coli strain DH5αPRO (Clontech, Mountain View, CA) was used throughout. *E. coli* expressing bla_{NDM-1} were created as described previously [51]. Briefly, bla_{NDM-1} was amplified from the plasmid pGDP1 NDM-1 plasmid (Addgene, Watertown, MA) and cloned into plasmid pPROLAR (origin of replication = p15a, selectable marker = kanamycin) using EcoR1 (New England Biolabs, Ipswich, MA) and HindIII (New England Biolabs). The resulting plasmid was sequenced and transformed into DH5αPRO. As a control, gfpmut(2b) was cloned into pPROLAR using EcoR1 and HindIII.

To create overnight cultures from which each experiment was initiated, single colonies were isolated from the lysogeny broth (LB) (MP Biomedical Santa Ana, CA) agar and inoculated into 3 mL of LB liquid medium with 50 μg/mL of kanamycin sulphate (ThermoFisher Scientific, Pittsburgh, PA) contained in 15 mL culture tubes (Genesee Scientific, Morrisville, NC). Overnight cultures were created by shaking the culture tubes at 37°C and 250 revolutions per minute for 24 hours.

All experiments were conducted in modified M9 medium [1X M9 salts (48 mM Na_2HPO_4, 22 mM KH_2PO_4, 862 mM NaCl, 19 mM NH_4Cl), 0.5% thiamine (Alfa Aesar, Ward Hill, MA), 2 mM $MgSO_4$, 0.1 mM $CaCl_2$], supplemented with 0.04% of each carbon source and varying concentrations of casamino acids (0.1%, 0.5% and 1%, Teknova, Hollister, CA) and isopropyl β-D-1-thiogalactopyranoside (IPTG, ThermoFisher). Carbon sources tested in this study were sodium acetate (Sigma Aldrich, St. Louis, MO), adenine (ThermoFisher), D-glucose (ThermoFisher), and D-ribose (ThermoFisher). Ampicillin sodium salt (ThermoFisher) was used to challenge *E. coli*.

Measuring ATP

We measured [ATP] using a previously published protocol [14]. Overnight cultures were diluted 1/40 into 40 mL of M9 medium in a 50 mL conical tube with the lid slightly unscrewed to allow gas exchange. The M9 medium contained IPTG but did not contain casamino acids and ampicillin. Bacteria were shaken for 2 hours at 250 RPM/37°C. Cultures were concentrated at least 2X (OD_{600} of > 0.05) in diluted (3:1) M9 medium that contained a carbon source (0.04%), IPTG (0, 0.1, 0.3, or 1mM) and casamino acids (0.1%, 0.5%, or 1%). 100 μL of these cultures were added to the wells of an opaque-walled 96-well plate (Costar 3370, Corning, Kennebunk, ME) in technical duplicate. The plate was covered with 2 BreathEasy (Sigma-Aldrich) membranes and placed in a shaker for 1 hour at 250 RPM/37°C. [ATP] was then measured using a BacterTiter-Glo microbial cell viability assay (Promega, Madison, WI) according to manufacturer recommendations and using a VICTOR X4

microplate reader (Perkin Elmer, Waltham, MA). Luminescence values were normalized to optical density (OD) at 600 nm (OD_{600}). [ATP] was determined using a standard curve produced using purified ATP [16].

Growth rate

Overnight cultures were resuspended in dH_2O. Each culture was diluted 200-fold into 200 μL of M9 medium (containing a carbon source, casamino acids, and IPTG) that was housed in a 96-well plate. The wells were overlaid with 70 μL of mineral oil to prevent evaporation. Cell density (OD_{600}) was measured every 10 minutes for 10 hours in a Victor X4 (Perkin Elmer) microplate reader preset to 37°C. OD_{600} values from cell-free medium were subtracted from all measurements. Maximum growth rate was determined from the experimental growth curves by fitting the data to a logistic growth equation as previously described [16].

MIC assays

Overnight cultures were resuspended in dH_2O and diluted to either high initial density ($5.3 \times 10^5 \pm 1.14 \times 10^5$ CFU/mL) or low initial density ($2.34 \times 10^4 \pm 2.88 \times 10^3$ CFU/mL, Wilcoxon: $P = 0.0051$, Shapiro-Wilk: $P = 0.0049$) into 200 μL of M9 medium housed in a 96-well plate (non-treated, Genesee Scientific) containing increasing concentrations of ampicillin and IPTG. The plates were sealed with two BreathEasy membranes (Sigma-Aldrich) and were placed in a shaker for 24 hours at 250 RPM and 37°C. After 24 hours, cell density (OD_{600}) was measured using a Victor NIVO plate reader (Perkin Elmer). Measurements that did not exceed 0.01 were set to zero, as values below this threshold are not reliable indicators of growth in our system [16]. MIC was determined as the lowest concentration of ampicillin that showed no growth. To assess the strength of IE (ΔMIC), we used the following equation:

$$\Delta MIC = MIC_{high\ density} - MIC_{low\ density}$$

Initial density was measured from overnight cultures using a dilution series followed by plating on LB agar containing 50 μg/mL of kanamycin. CFUs were enumerated after 20 hours of incubation at 37°C.

GFP expression

To measure the effect of increasing IPTG on expression of GFP, *gfp*-expressing *E. coli* were grown overnight, washed once with dH_2O and diluted 50-fold into 200 μL of M9 medium housed in a 96-well microplate (non-treated, Genesee Scientific). The microplate was covered with two BreathEasy films (Sigma-Aldrich), and shaken for 18 hours at 37 °C/RPM in a light-protected shaker. After 18 hours, GFP was measured in a Victor X4 microplate reader. GFP was normalized by OD_{600}. GFP signal produced by uninduced cultures was removed from all measurements. To determine any differences in GFP produced by high and low initial density populations, *gfp* expressing bacteria were grown as above, but diluted to high and low initial density into M9 medium as described in MIC assays. After 24 hours, GFP and OD_{600} were measured in a Victor X4 plate reader. GFP signal from no IPTG was subtracted from all measurements.

Mathematical modeling

We modified a previously published model to capture IE in the expression of β-lactamase [16].

$$\frac{dN}{dt} = (\mu - \epsilon)\left(1 - \frac{N}{N_m}\right)N - \left(\frac{N*A*\epsilon*b}{K+N*\beta}\right) \qquad \text{Eq. 1}$$

In our model, bacterial growth is captured using a logistic growth equation (left side). Bacterial growth depends upon two parameters: growth rate (μ ,/hr) of the bacteria and non-biomass generating metabolism (ε, mmol/g/hr), which approximates a maintenance coefficient. Bacteria (N, unitless) are initiated from one of two initial densities, high (N_{high}) or low (N_{low}), and grow to a fixed carrying capacity

(N_m, unitless). Antibiotics reduce logistic growth using a *per capita* death rate term (right side), which is modeled after Michaelis-Menten dynamics. The value of this term is dependent upon the bacterial density (N), the concentration of antibiotics (A, unitless), the half maximal rate of antibiotic-induced death (K, unitless), antibiotic lethality (b, /hr), metabolism (ε, mmol/g/hr), and the expression of β-lactamases (β, unitless). To account for the collective degradation of antibiotics by β-lactamases, we scaled β by N; the greater the bacterial density, the more β-lactamases are produced. This serves to reduce the impact of antibiotic lethality. To capture the metabolism-inducing increase of antibiotic lethality [14], A is scaled by ε. All simulations were performed for $t = 24$ hours using MATLAB (R2019b, MathWorks Inc., Natick, MA) using ode45.

We estimated the maximum value of growth rate (μ) using the average growth rate of *E. coli* in M9 medium (0.301 +/ - 0.003/hr) found in our experiments. We used previously reported maintenance coefficients (0.013-0.473 mmol/g/hr[52]) to estimate the order of magnitude of metabolism. To determine the range over which β-lactamase expression (β) could vary, we considered previously produced induction curves showing ~250-fold increase in luciferase activity as [IPTG] is increased from 0 mM to 1 mM and when driven by the $P_{lac\text{-}ara\text{-}1}$ promoter [36]. When $\beta = 1$, killing kinetics of the right-hand side of Eq. 1 are solely driven by the half maximal killing rate of the antibiotics (K) and cell density (N) in the denominator, capturing IE without an active form of resistance[16]. Thus, β values greater than 1 are required for β-lactamase expression in our model. Previously published time-kill curves showing that 0.1%-1% of bacteria survive after 3 hours in antibiotics provided at a concentration greater than MIC [14] were used to estimate the antibiotic killing rate (b). To capture the general trend of this range, we assumed a value of 0.1. The half-maximal killing rate of the antibiotic (K) was estimated by fitting the simulation results to the qualitative trends of our data. We estimated the initial density of the high and low initial density populations by assuming that the carrying capacity

of M9 medium with 0.04% glucose and 0.1% casamino acids was ~ 10^8 CFU/mL. Experimentally, the initial density of high and low populations in our study was determined to be 5.3 x 10^5 ± 1.14 x10^5 CFU/mL and 2.34 x 10^4 ± 2.88 x 10^3 CFU/mL, respectively. When normalized to a carrying capacity of 10^8 CFU/mL, this corresponded to initial densities that ranged from 10^{-2} to 10^{-3} and 10^{-3} to 10^{-4} for high and low density, respectively. We therefore set our initial density to 5 x 10^{-2} (N_{high}) and 1 x 10^{-4} (N_{low}), respectively, in our model. Sensitivity analysis for key model parameters is presented in Supplementary Fig. 4. All core parameters are listed in Supplementary Table 2; modifications to this parameter set are described throughout.

Statistical analysis

JMP (version 18.2.2, SAS Institute, Cary, NC) was used to test for significance throughout, including linear regression and Gaussian curve fitting. A Benjamini-Hochberg false discovery correction [53] was applied to all P values (including Shapiro-Wilk to test for normality) with a 0.05 false discovery rate. This resulted in a corrected significance cutoff value of $P \leq 0.0346$. This approach was chosen to apply a single correction across all P values, regardless of whether they are drawn from normally distributed or non-normally distributed populations. P values not directly reported in the figure legends or on the figure panels can be found in Supplementary Table 4.

References

1 Brook, I. Inoculum effect. *Reviews of infectious diseases* **11**, 361–368 (1989).

2 Tan, C. *et al.* The inoculum effect and band-pass bacterial response to periodic antibiotic treatment. *Molecular Systems Biology* **8**, 617 (2012). https://doi.org/10.1038/msb.2012.49

3 Lenhard, J. R. & Bulman, Z. P. Inoculum effect of β-lactam antibiotics. *Journal of Antimicrobial Chemotherapy* **74**, 2825–2843 (2019).

4 Smith, K. P. & Kirby, J. E. The inoculum effect in the era of multidrug resistance: minor differences in inoculum have dramatic effect on MIC determination. *Antimicrobial agents and chemotherapy* **62**, 10.1128/aac. 00433–00418 (2018).

5 Jean, B. *et al.* β-Lactam Inoculum Effect in Methicillin-Susceptible Staphylococcus aureus Infective Endocarditis. *JAMA Netw Open* **7**, e2451353 (2024). https://doi.org/10.1001/jamanetworkopen.2024.51353

6 Miller, W. R. *et al.* The Cefazolin Inoculum Effect Is Associated With Increased Mortality in Methicillin-Susceptible Staphylococcus aureus Bacteremia. *Open Forum Infectious Diseases* **5**, ofy123 (2018). https://doi.org/10.1093/ofid/ofy123

7 Lee, S. *et al.* Clinical implications of cefazolin inoculum effect and β-lactamase type on methicillin-susceptible Staphylococcus aureus bacteremia. *Microbial Drug Resistance* **20**, 568–574 (2014).

8 Martinez, J. & Baquero, F. Mutation frequencies and antibiotic resistance. *Antimicrob Agents Chemother* **44**, 1771–1777 (2000).

9 Fantin, B. *et al.* The inoculum effect of Escherichia coli expressing mcr-1 or not on colistin activity in a murine model of peritonitis. *Clinical Microbiology and Infection* **25**, 1563. e1565–1563. e1568 (2019).

10 Eagle, H. The effect of the size of the inoculum and the age of the infection on the curative does of penicillin in experimental infections with Streptococci, Pneumococci and Treponema pallidum. *The Journal of Experimental Medicine* **90**, 595–607 (1949). https://doi.org/10.1084/jem.90.6.595

11 Ahmad, M., Aduru, S. V., Smith, R. P., Zhao, Z. & Lopatkin, A. J. The role of bacterial metabolism in antimicrobial resistance. *Nature Reviews Microbiology*, 1–16 (2025).

12 Tuomanen, E., Cozens, R., Tosch, W., Zak, O. & Tomasz, A. The rate of killing of Escherichia coli by beta-lactam antibiotics is strictly proportional to the rate of bacterial growth. *J Gen Microbiol* **132**, 1297–1304 (1986). https://doi.org/10.1099/00221287-132-5-1297

13 Łapińska, U. *et al.* Fast bacterial growth reduces antibiotic accumulation and efficacy. *Elife* **11**, e74062 (2022).

14 Lopatkin, A. J. *et al.* Bacterial metabolic state more accurately predicts antibiotic lethality than growth rate. *Nature microbiology* **4**, 2109–2117 (2019).

15 Hernandez, D. M. *et al.* Purine and pyrimidine synthesis differently affect the strength of the inoculum effect for aminoglycoside and B-lactam antibiotics. *bioRxiv*, 2024.2004. 2009.588696 (2024).

16 Diaz-Tang, G. *et al.* Growth productivity as a determinant of the inoculum effect for bactericidal antibiotics. *Science Advances* **8**, eadd0924 (2022).

17 Tooke, C. L. *et al.* β-Lactamases and β-Lactamase Inhibitors in the 21st Century. *Journal of molecular biology* **431**, 3472–3500 (2019).

18 Wikler, M. A. Performance standards for antimicrobial susceptibility testing Sixteenth informational supplement. *M 100-S 16* (2006).

19 McNeil, J. C. *et al.* Cefazolin inoculum effect and methicillin-susceptible Staphylococcus aureus osteoarticular infections in children. *Antimicrob Agents Chemother* **64**, e00703–00720 (2020).
20 Betriu, C. *et al.* Comparative in vitro activity and the inoculum effect of ertapenem against Enterobacteriaceae resistant to extended-spectrum cephalosporins. *Int J Antimicrob Agents* **28**, 1–5 (2006).
21 Wu, G. *et al.* Metabolic burden: cornerstones in synthetic biology and metabolic engineering applications. *Trends in biotechnology* **34**, 652–664 (2016).
22 Na, Y.-A. *et al.* Growth retardation of Escherichia coli by artificial increase of intracellular ATP. *Journal of Industrial Microbiology and Biotechnology* **42**, 915–924 (2015).
23 Rajer, F. & Sandegren, L. The role of antibiotic resistance genes in the fitness cost of multiresistance plasmids. mBio 13: e0355221. *DOI* **10**, 03552–03521 (2022).
24 Marciano, D. C., Karkouti, O. Y. & Palzkill, T. A fitness cost associated with the antibiotic resistance enzyme SME-1 β-lactamase. *Genetics* **176**, 2381–2392 (2007).
25 Smith, R. P. *et al.* The public and private benefit of an impure public good determines the sensitivity of bacteria to population collapse in a snowdrift game. *Environmental microbiology* **21**, 4330–4342 (2019).
26 Thomson, K. S. & Moland, E. S. Cefepime, piperacillin-tazobactam, and the inoculum effect in tests with extended-spectrum β-lactamase-producing Enterobacteriaceae. *Antimicrob Agents Chemother* **45**, 3548–3554 (2001).
27 Meredith, H. R., Srimani, J. K., Lee, A. J., Lopatkin, A. J. & You, L. Collective antibiotic tolerance: mechanisms, dynamics and intervention. *Nature Chemical Biology* **11**, 182–188 (2015).
28 Geyrhofer, L. *et al.* Minimal Surviving Inoculum in Collective Antibiotic Resistance. *mBio* **14**, e0245622 (2023). https://doi.org/10.1128/mbio.02456-22
29 Artemova, T., Gerardin, Y., Dudley, C., Vega, N. M. & Gore, J. Isolated cell behavior drives the evolution of antibiotic resistance. *Molecular systems biology* **11**, 822 (2015).
30 De Vos, M. G., Zagorski, M., McNally, A. & Bollenbach, T. Interaction networks, ecological stability, and collective antibiotic tolerance in polymicrobial infections. *Proceedings of the National Academy of Sciences* **114**, 10666–10671 (2017).
31 Lee, S. H. *et al.* Association between type A blaZ gene polymorphism and cefazolin inoculum effect in methicillin-susceptible Staphylococcus aureus. *Antimicrobial Agents and Chemotherapy* **60**, 6928–6932 (2016).
32 Lee, S. O., Lee, S., Park, S., Lee, J. E. & Lee, S. H. The cefazolin inoculum effect and the presence of type A blaZ gene according to agr genotype in methicillin-susceptible Staphylococcus aureus bacteremia. *Infection & Chemotherapy* **51**, 376 (2019).
33 Nannini, E. C. *et al.* Determination of an inoculum effect with various cephalosporins among clinical isolates of methicillin-susceptible Staphylococcus aureus. *Antimicrobial agents and chemotherapy* **54**, 2206–2208 (2010).
34 Craig, W. A., Bhavnani, S. M. & Ambrose, P. G. The inoculum effect: fact or artifact? *Diagnostic microbiology and infectious disease* **50**, 229–230 (2004).
35 Yong, D. *et al.* Characterization of a new metallo-β-lactamase gene, bla NDM-1, and a novel erythromycin esterase gene carried on a unique genetic structure in Klebsiella pneumoniae sequence type 14 from India. *Antimicrobial agents and chemotherapy* **53**, 5046–5054 (2009).
36 Lutz, R. & Bujard, H. Independent and tight regulation of transcriptional units in Escherichia coli via the LacR/O, the TetR/O and AraC/I1-I2 regulatory elements. *Nucleic acids research* **25**, 1203–1210 (1997).

37 Khan, A. U., Maryam, L. & Zarrilli, R. Structure, genetics and worldwide spread of New Delhi metallo-β-lactamase (NDM): a threat to public health. *BMC microbiology* **17**, 101 (2017).
38 Hempfling, W. P. & Mainzer, S. E. Effects of varying the carbon source limiting growth on yield and maintenance characteristics of Escherichia coli in continuous culture. *Journal of bacteriology* **123**, 1076–1087 (1975).
39 Marr, A. G. Growth rate of Escherichia coli. *Microbiological reviews* **55**, 316–333 (1991).
40 Rouches, M. V., Xu, Y., Cortes, L. B. G. & Lambert, G. A plasmid system with tunable copy number. *Nature communications* **13**, 3908 (2022).
41 Fridman, O., Goldberg, A., Ronin, I., Shoresh, N. & Balaban, N. Q. Optimization of lag time underlies antibiotic tolerance in evolved bacterial populations. *Nature* **513**, 418–421 (2014).
42 Snoeck, S., Guidi, C. & De Mey, M. "Metabolic burden" explained: stress symptoms and its related responses induced by (over) expression of (heterologous) proteins in Escherichia coli. *Microbial Cell Factories* **23**, 96 (2024).
43 Weber, J., Li, Z. & Rinas, U. Recombinant protein production provoked accumulation of ATP, fructose-1, 6-bisphosphate and pyruvate in E. coli K12 strain TG1. *Microbial Cell Factories* **20**, 169 (2021).
44 Yang, J. H. *et al.* Antibiotic-induced changes to the host metabolic environment inhibit drug efficacy and alter immune function. *Cell host & microbe* **22**, 757–765. e753 (2017).
45 Meylan, S. *et al.* Carbon sources tune antibiotic susceptibility in Pseudomonas aeruginosa via tricarboxylic acid cycle control. *Cell chemical biology* **24**, 195–206 (2017).
46 Bourreau, A., Le Mabecque, V., Broquet, A. & Caillon, J. Prevalence of a cefazolin inoculum effect associated with blaZ gene types, and clinical outcomes among methicillin-susceptible Staphylococcus aureus blood isolates of patients with infective endocarditis. *Infectious Diseases Now* **53**, 104626 (2023).
47 Jean, B. *et al.* β-Lactam Inoculum Effect in Methicillin-Susceptible Staphylococcus aureus Infective Endocarditis. *JAMA Network Open* **7**, e2451353–e2451353 (2024).
48 Miller, W. R. *et al.* in *Open forum infectious diseases.* ofy123 (Oxford University Press US).
49 Guo, J. *et al.* Implications of pH and Ionic Environment in Chronic Diabetic Wounds: An Overlooked Perspective. *Clin Cosmet Investig Dermatol* **17**, 2669–2686 (2024). https://doi.org/10.2147/ccid.S485138
50 Mann, R., Mediati, D. G., Duggin, I. G., Harry, E. J. & Bottomley, A. L. Metabolic Adaptations of Uropathogenic E. coli in the Urinary Tract. *Front Cell Infect Microbiol* **7**, 241 (2017). https://doi.org/10.3389/fcimb.2017.00241
51 Palomino, A. *et al.* Metabolic genes on conjugative plasmids are highly prevalent in Escherichia coli and can protect against antibiotic treatment. *The ISME Journal* **17**, 151–162 (2023).
52 Wallace, R. J. & Holms, W. H. Maintenance coefficients and rates of turnover of cell material in Escherichia coli ML308 at different growth temperatures. *FEMS Microbiol Lett* **37**, 317–320 (1986).
53 Benjamini, Y. & Hochberg, Y. The adaptive control of the false discovery rate in multiple comparison problems. *J Educ Behav Stat* **25**, 60–83 (2000).

Author contributions

Conceptualization -RPS
Formal analysis –ARKT, RPS
Funding acquisition – RPS and AJL
Investigation – ARKT, KS, PI, TM, NN, JG, TR, DPM, DW, TW, AP, RPS
Methodology - ARKT
Project administration - RPS
Supervision - RPS
Visualization – ARKT, RPS
Writing – original draft - ARKT, RPS
Writing – review & editing - ARKT, KS, PI, TM, NN, JG, TR, DPM, DW, TW, AP, AJL

Conflict of interest

The authors declare that they do not have any conflicts of interest.

Data access

All data associated with this manuscript can be found on figshare at the following address:

https://figshare.com/s/3d0cd955a9bda863cec8

Funding statement

This work was supported by National Institutes of Health grant R15AI159902 (RPS) and National Institutes of Health grant 1R35GM150871-01 (AJL). Images were created using Biorender.

Figures and Figure Legends

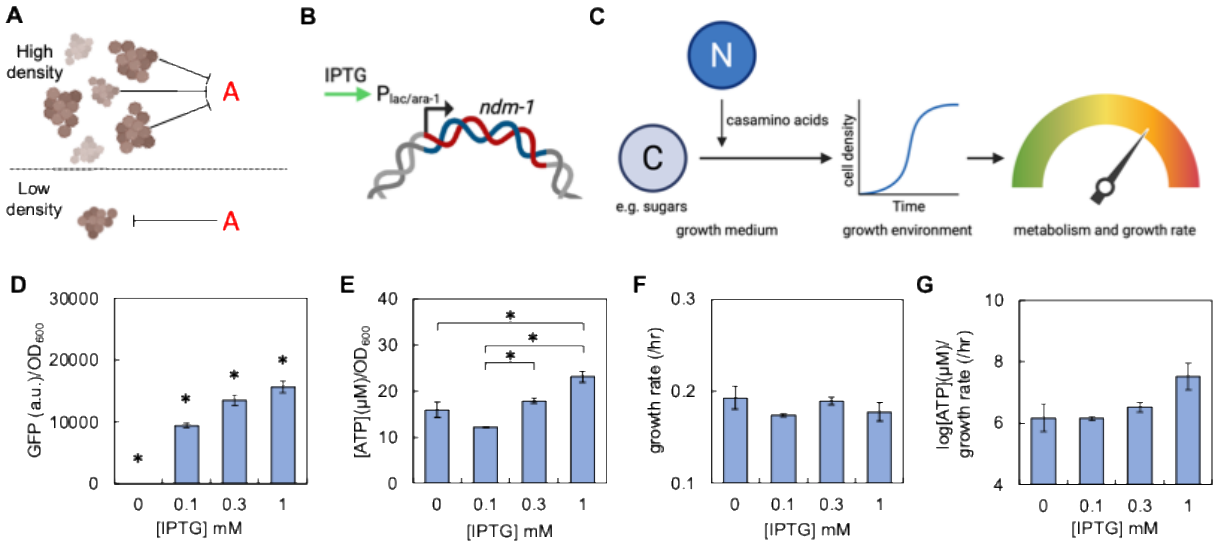

Figure 1: Expression of β-lactamase changes [ATP] and growth rate in *E. coli.*

A) The inoculum effect. At high density, the bacterial population resists the antibiotic (*A*) and grows. Otherwise, at low initial density, the bacterial population is susceptible to the antibiotic and dies.

B) We used *E. coli* expressing the NDM-1 β-lactamase from a plasmid. Expression was regulated using an IPTG-inducible $P_{lac/ara-1}$ promoter.

C) Manipulating bacterial metabolism ([ATP]) and growth rate. The carbon source in the growth medium defined the growth environment. Varying the nitrogen source (casamino acids) varies [ATP] and growth rate for a given growth environment.

D) Increasing [IPTG] increased the expression of downstream elements. Green fluorescent protein (GFP, arbitrary units, a.u.) was normalized by cell density (OD_{600}). * = all comparisons were significantly different (Kruskal-Wallis: $P < 0.0001$, (Shapiro Wilk: $P = 0.0002$); Wilcoxon: $P \leq 0.013$). For panels D-G, the standard error of the mean (SEM) is calculated from ≥ 3 biological replicates. Raw data in Supplementary Fig. 1.

E) Effect of increasing [IPTG] on [ATP] production. [ATP] was normalized by cell density (OD_{600}). * = significantly different (Kruskal-Wallis: $P < 0.0001$ (Shapiro Wilk: $P < 0.0001$); Wilcoxon: $P \leq 0.0094$).

F) Effect of increasing [IPTG] on growth rate. None of the growth rates were significantly different. Average residuals for curve fitting in Supplementary Table 1.

G) The ratio of log[ATP]/growth rate as a function of increasing [IPTG]. [ATP] and growth rate from panels E and F.

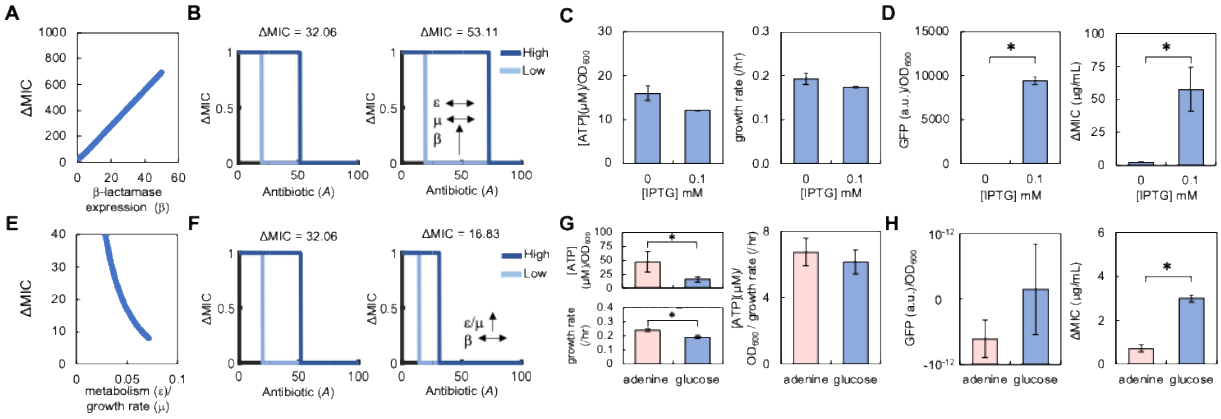

Figure 2: A simple mathematical model predicts experimentally verified changes to ΔMIC.

A) Simulations predict that increasing β-lactamase expression (*β*) increases ΔMIC. For all simulations, $t = 24$ hours. Justification of parameters in *Methods*; values used for simulations in Supplementary Table 2.

B) Increasing β-lactamase (*β*) expression from 1 (left) to 3 (right) increases ΔMIC.

C) Experiment: Left: [ATP] normalized by cell density for *E. coli* grown in medium with glucose and with either 0 or 0.1 mM IPTG. Right: Growth rate for *E. coli* grown in medium with glucose and with either 0 or 0.1 mM IPTG. For both panels, SEM from ≥ 3 biological replicates.

D) Experiments: Left: GFP normalized by cell density for *E. coli* grown in medium with glucose and with either 0 or 0.1 mM IPTG. * = significantly different (Wilcoxon: $P < 0.0001$; Shapiro Wilk: $P < 0.0001$)). Right: ΔMIC *E. coli* grown in medium with glucose and with either 0 or 0.1 mM IPTG. * = significantly different (Wilcoxon: $P < 0.0001$; Shapiro Wilk: $P < 0.0001$). For both panels, SEM from 6 biological replicates. Raw MIC data in Supplementary Fig. 3.

E) Simulations predict that increasing metabolism (*ε*) / growth rate (μ) decreases ΔMIC.

F) Increasing metabolism (*ε*) / growth rate (μ) from 0.033 (left) to 0.05 (right) decreases ΔMIC.

G) Experiment: Left, top: [ATP] normalized by cell density for *E. coli* grown in medium with adenine or glucose with 0 mM IPTG. Left, bottom: Growth rate for *E. coli* grown in medium with adenine or glucose with 0 mM IPTG. For both panels, SEM from ≥ 3 biological replicates. * = significantly different ($P < 0.0001$, one-tailed t-test). Right: [ATP]/growth rate determined from left panels.

H) Experiments: Left: GFP normalized by cell density for *E. coli* grown in medium with adenine or glucose and with 0 mM IPTG. Right: ΔMIC *E. coli* grown in medium with adenine or glucose and with 0 IPTG. * = significantly different (one-tailed t-test: $P = 0.017$). For both panels, SEM from 6 biological replicates.

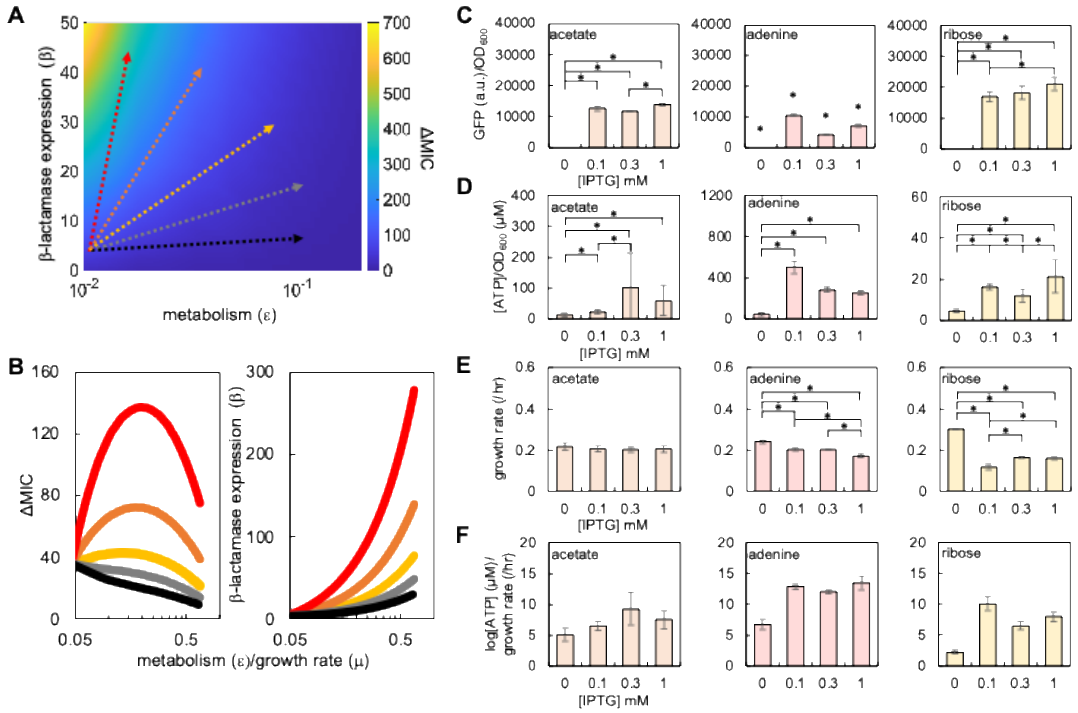

Figure 3: A metabolism-growth landscape reveals a biphasic relationship between ΔMIC, metabolism, and growth rate.

A) Simulated heat map showing the effect of increasing metabolism (ε) and β-lactamase expression (*β*) on ΔMIC. Growth rate (*μ*) held constant. The arrows indicate an approximate slice of the heat map, revealing relationships between ε/μ and ΔMIC for different values of β, as shown in panel B. Sensitivity analysis, including the removal of *ε* from the *per capita* death rate term (Eq. 1), is presented in Supplementary Fig. 4.

B) Left: Simulations showing the effect of increasing metabolism (ε) and β-lactamase expression (β) on the relationship with ΔMIC. Colors match arrows in panel A. Right: Simulations showing the value of β-lactamase expression (β) for each value of metabolism (ε)/growth rate (μ) in the left panel.

C) GFP expression in *E. coli* grown in M9 medium with different carbon sources and [IPTG]. GFP was normalized by cell density (OD_{600}). GFP signal from no IPTG was subtracted from all measurements. * = significantly different (Kruskal-Wallis: $P < 0.0001$ (Shapiro Wilk: $P = 0.0137$), Wilcoxon: $P \leq 0.0142$). For panels C-F, SEM from ≥ 3 biological replicates. Raw data in Supplementary Fig. 5.

D) [ATP] for *E. coli* grown in M9 medium with different carbon sources and [IPTG]. * = significantly different (Kruskal-Wallis: $P < 0.0001$ (Shapiro Wilk: $P < 0.0001$), Wilcoxon: $P \leq 0.0193$)).

E) Growth rate of *E. coli* grown in M9 medium with different carbon sources and [IPTG]. * = significantly different (Kruskal-Wallis: $P < 0.0001$ (Shapiro Wilk: $P = 0.0154$), Wilcoxon: $P \leq 0.0193$)). Average residuals for curve fitting in Supplementary Table 3; growth curves in Supplementary Fig. 5.

F) The effect of changing the carbon source in the growth medium on log[ATP]/growth rate. [ATP] and growth rate from panels D and E, respectively.

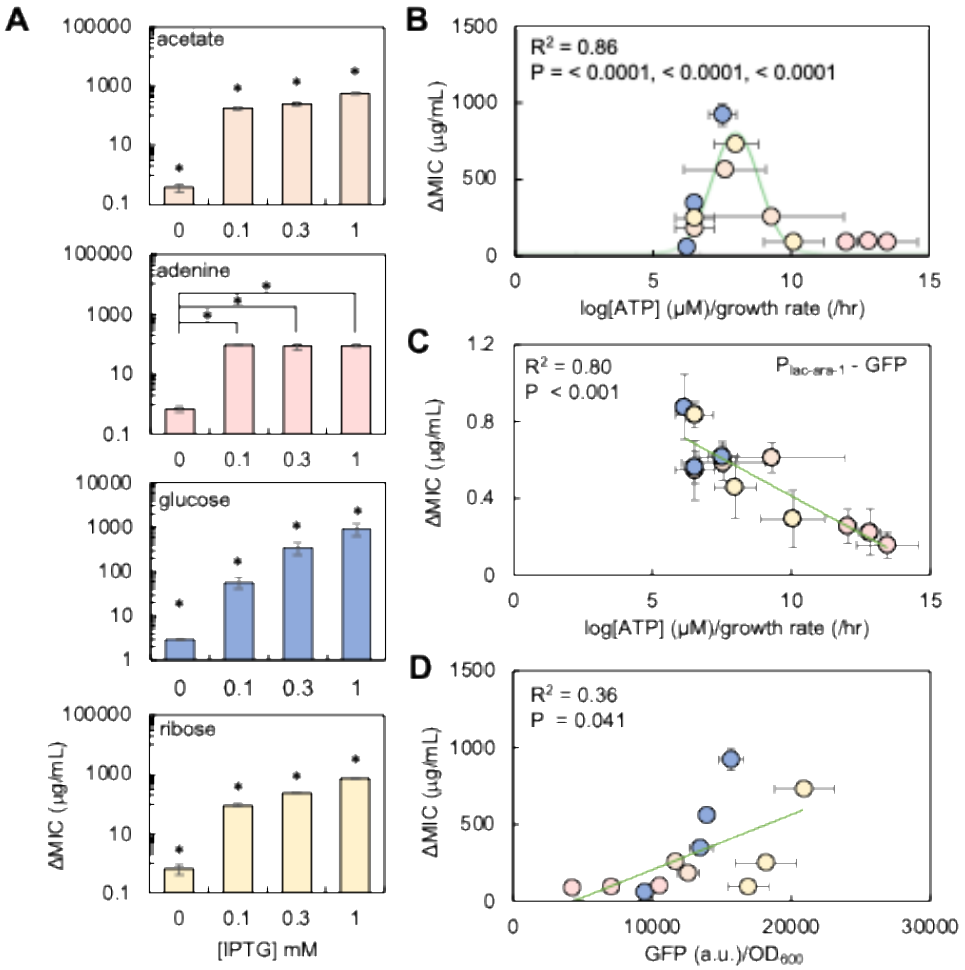

Figure 4: ΔMIC and log[ATP]/growth rate follow a biphasic trend when *E. coli* express the NDM-1 β-lactamase.

A) ΔMIC as a function of [IPTG] for NDM-1expressing *E. coli* grown in M9 medium with different carbon sources as indicated. SEM from ≥ 4 biological replicates. * = significantly different (Kruskal-Wallis: $P < 0.0001$ (Shapiro Wilk: $P < 0.0001$), Wilcoxon: $P \leq 0.0286$). For acetate, glucose, and ribose, all comparisons were significantly different; only those indicated for adenine were significantly different. Raw data in Supplementary Fig. 6.

B) ΔMIC as a function of log[ATP]/growth rate. P values (in order – peak value, critical point, growth rate) and R^2 value from a Gaussian fit. ΔMIC from panel A; log[ATP]/growth rate from Fig. 3F. For panels B-D, colored data points correspond with the color scheme in panel A and only conditions with [IPTG] in medium leading to β-lactamase expression are plotted.

C) ΔMIC as a function of log(ATP)/growth rate for *E. coli* expressing GFP. log(ATP)/growth rate from Fig. 3F. SEM from 6 biological replicates. R^2 and P value from linear regression. Raw data in Supplementary Fig. 7.

D) ΔMIC as a function of GFP/OD_{600} rate for *E. coli* expressing GFP grown in different carbon sources. SEM from 6 biological replicates. R^2 and P value from linear regression.

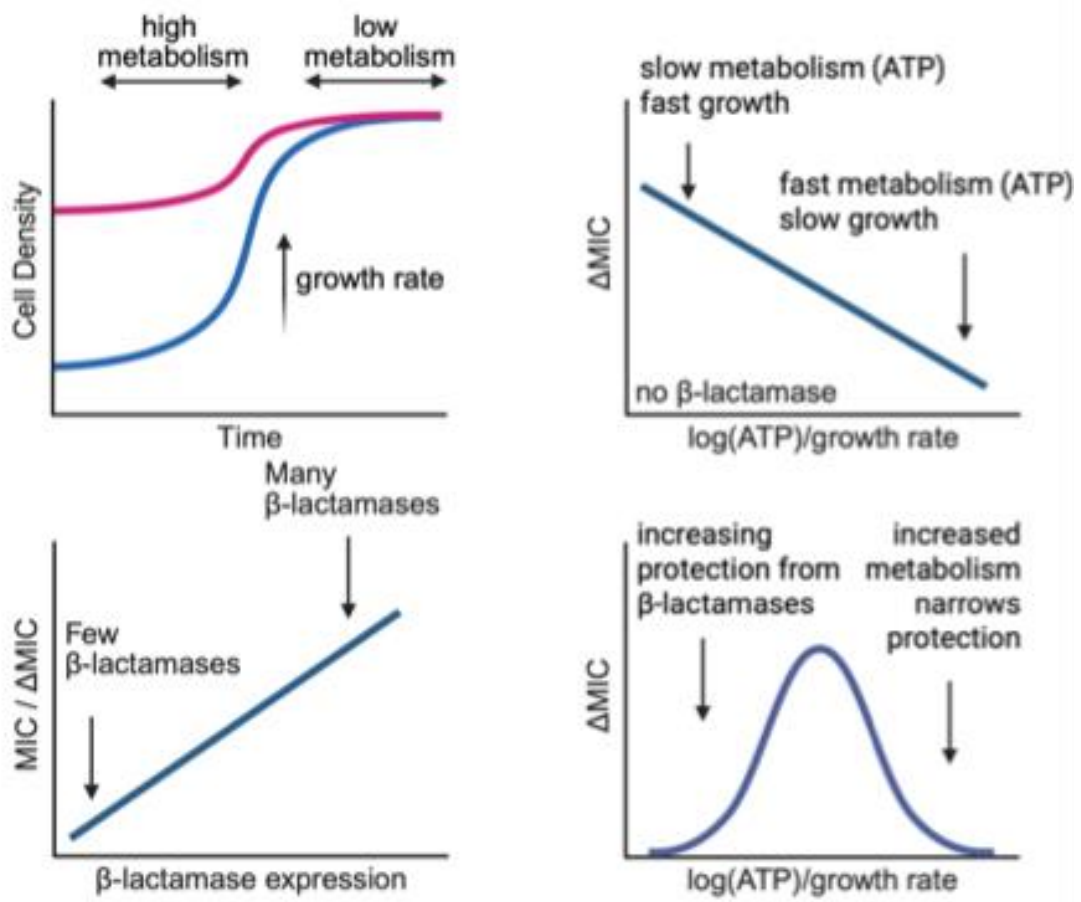

Figure 5: Our proposed mechanism to explain the biphasic dependence of ΔMIC on log[ATP]/growth rate.

A) The initial density of a bacterial population determines how long it spends in log phase growth, where metabolism is greater. The growth rate afforded to the population dictates how long it takes for the population to reach the stationary phase, where metabolism is reduced.

B) When growth is relatively greater than metabolism (e.g., ATP), the difference in MIC between both populations is increased as the high-density population spends a relatively shorter time in log phase growth, where antibiotic lethality is maximized. This increases ΔMIC. When [ATP] is greater than growth, the time at which both populations have high metabolism becomes increasingly similar, leading to similar MICs between them. This reduces ΔMIC.

C) Independent of changes in metabolism and growth, increasing β-lactamase expression increases ΔMIC; the more β-lactamases available, the more the population collectively inactivates β-lactams.

D) The biphasic relationship between ΔMIC and [ATP]/growth rate observed in our study. On the left side of the curve, increasing β-lactamase expression increases ΔMIC. Owing to low metabolism relative to growth, the difference in ΔMIC between high and low density populations is increased. On the right side of the curve, increases in metabolism relative to growth allow both the high- and low-density populations to inactivate similar amounts of β-lactam antibiotics, reducing the difference in MIC and leading to lower ΔMIC.